ISBN: 978-3-95450-236-3 ISSN: 2673-5350 doi:10.18429/JACoW-IBIC2023-MOP041

MODIFIED FAST ORBIT FEEDBACK CONTROLLER FOR DISTURBANCE ATTENUATION IN LONG STRAIGHTS FOR DIAMOND-II *

S. Banerjee[1,†], I. Kempf[1,2], M. Abbott[1], L. Bobb[1],
[1] Diamond Light Source, Didcot, United Kingdom
[2] University of Oxford, Oxford, United Kingdom

Abstract

At Diamond Light Source, the fast orbit feedback (FOFB) uses one array of correctors and the controller is designed using the internal model control (IMC) structure. The Diamond-II upgrade will introduce an additional array of fast correctors and a new controller that is designed using the generalised modal decomposition, increasing the overall closed-loop bandwidth from 140 Hz to 1 kHz. Although simulation results have shown that the resulting beam displacement is within specification in all straights, they have also shown that the performance on long straights is limited, particularly in the vertical plane. In this paper, the controller is tuned in order to increase the FOFB performance in long straights by introducing a mode-by-mode regularisation parameter. The performance of the controller beyond 1 kHz is assessed using new disturbance data and a new measurement noise model, showing that the Diamond-II performance criteria are met, even in the presence of measurement noise.

INTRODUCTION

At Diamond Light Source (Diamond), the fast orbit feedback (FOFB) attenuates disturbances in the storage ring and reduces the root-mean square deviation of the electron beam to ≤10 % of the beam size up to 140 Hz in both planes. The FOFB uses 173 beam position monitors (BPMs) and 172 identical corrector magnets, and the control algorithm is based on the internal model control (IMC) structure, which is naturally amenable to systems with large time delays. The controller is designed using the modal decomposition, which decouples the multi-input multi-output (MIMO) systems into sets of single-input single-output systems using the singular value decomposition (SVD) of the orbit response matrix (ORM) [1].

Due to advances in detector speed and resolution at Diamond-II [2], the beam stability requirements are raised to 3 % of the beam size up to 1 kHz, such as shown in Table 1. The increased closed-loop bandwidth in turn requires to introduce an additional corrector type. The FOFB at Diamond-II will use 252 slow correctors with a bandwidth of ∼ 200 Hz and 144 fast correctors with a bandwidth of ∼ 8 kHz. To accommodate the fast correctors, the Diamond FOFB controller has been extended and adapted to the Diamond-II configuration [3]. Analogous to Diamond, the MIMO system is decoupled into sets of two-input single-output (TISO) and SISO systems using the generalised singular value decomposition (GSVD), which is a two-matrix factorisation technique [4]. The decoupled systems are then embedded in the IMC structure and the controllers designed using mid-ranging control [5]. In addition, a tunable regularisation matrix is included in the feedback loop to avoid large control inputs and increase the robustness of the controller.

Table 1: Beam Size, Relative and Absolute Orbit Stability Requirements at Standard Straight Source Points [2].

Parameter	Diamond	Diamond-II
Beam size H/V	123 µm/3.5 µm	30 µm/4 µm
Rel. stability	10 % up to 100 Hz	3 % up to 1 kHz
Abs. stability H/V	12 µm/0.35 µm	0.9 µm/0.12 µm

H: horizontal, V: vertical, BW: bandwidth

As part of the Diamond-II design, the performance of the new control algorithm has been assessed using estimates of the Diamond-II disturbance [6]. Although this has shown that the Diamond-II controller meets the beam stability requirements, it has also shown that the performance for primary BPMs on the long straights of the new multi-bend achromat (MBA) lattice is worse than on the standard straights and mid straights. To reduce this performance difference, this paper extends the approach presented in [3] by introducing mode-based weights for the regularisation matrix, increasing the control effort for primary BPMs on long straights. The performance of the FOFB is then reassessed, considering both disturbance and a new measurement noise model.

DISTURBANCE

The Diamond-II disturbance data presented in Ref. [6] has been extended from 1 kHz to 2.44 kHz. The data includes power spectral density (PSD) estimates of ground and girder vibrations, RF and power supply noise, and is scaled using the local beta function to obtain the disturbance profile at each BPM, such as shown in Fig. 1 for the upstream primary BPM of the first standard straight, which is comparable to primary BPMs in other straight.

Note that the PSDs from Fig. 1 lack phase information, which complicates the analysis of the MIMO system. Since the ORMs are ill-conditioned, most of the measured disturbance is concentrated in the modes associated with large singular values of the ORMs. However, this is not reflected in the PSDs from Fig. 1, and therefore impacts the performance estimation of the MIMO system.

* Work supported by Diamond Light Source
† Corresponding author: shohan.banerjee@diamond.ac.uk.

ISBN: 978-3-95450-236-3 ISSN: 2673-5350 doi:10.18429/JACoW-IBIC2023-MOP041

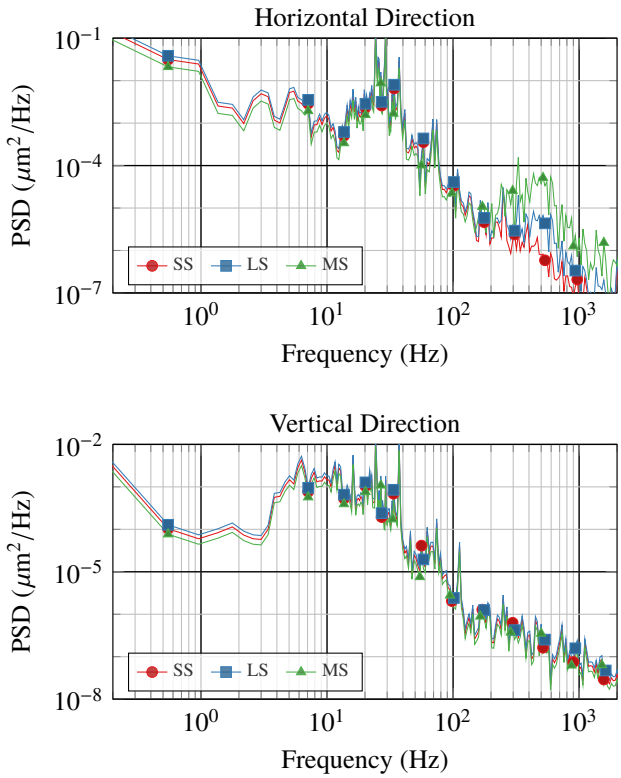

Figure 1: Estimated power spectral densitiy (PSD) of the uncorrected horizontal and vertical disturbance for Diamond-II at primary BPMs on long straights (LS), standard straights (SS), and mid straights (MS). The values are averaged over upstream and downstream BPMs.

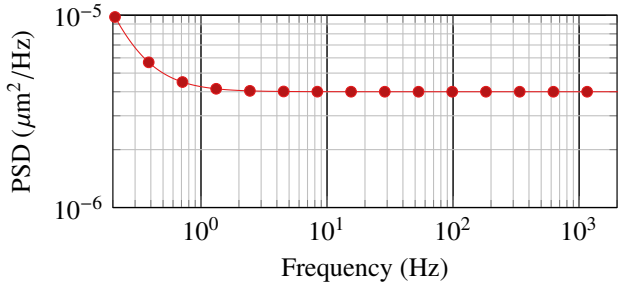

Figure 2: Power spectral densitiy (PSD) obtained from the Diamond-II measurement noise model.

MEASUREMENT NOISE

The FOFB at Diamond-II will also use new BPMs [7], and this reassessment includes a new measurement noise model. The PSD of the measurement noise is assumed to be $N(\omega) := \alpha^2/\omega^2 + \beta^2$, where $\alpha := 0.5\,\mathrm{nm}/\sqrt{\mathrm{Hz}}$ and $\beta := 2\,\mathrm{nm}/\sqrt{\mathrm{Hz}}$ are chosen based on the BPM specifications for Diamond-II. Figure 2 shows the resulting PSD, which is used for both horizontal and vertical directions. Comparing with Fig. 1, the PSD of the measurement noise is several orders of magnitude lower than the PSD of the disturbance for frequencies below 100 Hz, of similar magnitude between 100 Hz and 1 kHz, and represents a significant contribution from 1 kHz on.

CONTROLLER

The electron beam dynamics at Diamond-II are

$$y(s) = R_\mathrm{s} g_\mathrm{s}(s) u_\mathrm{s}(s) + R_\mathrm{f} g_\mathrm{f}(s) u_\mathrm{f}(s) + d(s), \qquad (1)$$

where the s is the Laplace variable and the subscripts s and f refer to slow and fast. The vectors $y(s)$, $u_{(\cdot)}(s)$ and $d(s)$ represent the beam position, the corrector inputs, and the disturbances, respectively, and the matrices $R_\mathrm{s} \in \mathbb{R}^{n_y \times n_\mathrm{s}}$ and $R_\mathrm{f} \in \mathbb{R}^{n_y \times n_\mathrm{f}}$ with $n_y = n_\mathrm{s} = 252$ and $n_\mathrm{f} = 144$ the ORMs for the slow and fast correctors, which are obtained from selecting the corresponding columns of a larger ORM $R \in \mathbb{R}^{n_y \times (n_\mathrm{s}+n_\mathrm{f})}$. The scalar transfer functions $g_\mathrm{s}(s)$ and $g_\mathrm{f}(s)$ model the temporal dynamics of the correctors, and include the frequency responses of the DAC, ADC, signal processing filters, power supplies, magnets, and copper vessel for slow correctors and stainless steel and copper vessel for fast correctors.

The IMC structure used for Diamond-II is shown in Fig. 3, where $P(s) := [R_\mathrm{s} g_\mathrm{s}(s)\ R_\mathrm{f} g_\mathrm{f}(s)]$ is the plant, $\bar{P}(s) := [\bar{R}_\mathrm{s} \bar{g}_\mathrm{s}(s)\ \bar{R}_\mathrm{f} \bar{g}_\mathrm{f}(s)]$ the plant model, $Q(s) := \mathrm{diag}(Q_\mathrm{s}(s), Q_\mathrm{f}(s))$ the IMC filter, $u(s) := [u_\mathrm{s}(s)^\mathrm{T}\ u_\mathrm{f}(s)^\mathrm{T}]^\mathrm{T}$, and $n(s)$ is the measurement noise. Note that $n(s)$ affects $y(s)$ when the control loop is closed, i.e. when $us(s)$ and $uf(s)$ in Eq. (1) are replaced with a control law that uses the measured position $y(s) + n(s)$.

The IMC filters invert the plant and are defined as $Q_{(\cdot)}(s) := P^\dagger_{(\cdot)}(s) T_{(\cdot)}(s)$, $(\cdot) = \{\mathrm{s}, \mathrm{f}\}$, where it is assumed that $\bar{P}(s) = P(s)$ and $T_{(\cdot)}(s)$ are tunable transfer functions designed in the companion paper [8]. The matrix $\Upsilon \in \mathbb{R}^{(n_\mathrm{s}+n_\mathrm{f}) \times n_y}$ is used to accommodate systems with fewer slow than fast correctors, and the matrix $\Gamma \in \mathbb{R}^{n_y \times n_y}$ is the regularisation matrix that is defined as

$$\begin{aligned} \Gamma &:= (RR^\mathrm{T} + \mu I)^{-1} RR^\mathrm{T} \\ &= U\,\mathrm{diag}\left(\frac{\sigma_1^2}{\sigma_1^2 + \mu}, \ldots, \frac{\sigma_{n_y}^2}{\sigma_{n_y}^2 + \mu} \right) U^\mathrm{T} \end{aligned} \qquad (2)$$

where $\mu \geq 0.1$ the regularisation parameter and the SVD $R = U\Sigma V^\mathrm{T}$ was substituted for R. Given $T_{(\cdot)}(s)$, the choice of μ influences both closed-loop bandwidth and corrector demand. A large value of μ ($\mu \gg \sigma_{n_y}$) reduces both closed-loop bandwidth and corrector demand, but a small value of μ can yield large corrector inputs and even an unstable closed-loop [9]. The choice $\mu = 0.1$ results in a maximum fast corrector demand of 276 mA, which is below the limit of 920 mA [2].

MODE-BY-MODE REGULARISATION

As for Diamond, the Diamond-II ORMs are ill-conditioned, i.e. the ratio of largest to smallest singular value is large. Because the IMC filters invert the plant, the corrector inputs are proportional to $R^\dagger_{(\cdot)}$, producing large corrector inputs for disturbances in the direction of standard singular vectors associated with small singular values of $R^\dagger_{(\cdot)}$. While the regularisation matrix Γ is used to reduce the

ISBN: 978-3-95450-236-3 ISSN: 2673-5350 doi:10.18429/JACoW-IBIC2023-MOP041

Table 2: Targets and expected IBMs up to 1 kHz for Diamond-II at primary BPMs on long straights (LS), mid straights (MS), and standard straights (SS). The values are averaged over upstream and downstream BPMs.

	Noise	μ_i	Horizontal IBM (µm)			Vertical IBM (µm)		
			LS	MS	SS	LS	MS	SS
Target			1.20	0.90	0.97	0.23	0.14	0.18
FOFB OFF	No		0.68	0.46	0.61	0.25	0.20	0.21
Upper bound from Eq. (6)	No	0.1	0.48	0.23	0.35	0.25	0.09	0.12
Simulation	No	0.1	0.17	0.06	0.08	0.17	0.05	0.07
Upper bound from Eq. (6)	No	$f(\theta_i)$	0.48	0.23	0.35	0.26	0.09	0.12
Simulation	No	$f(\theta_i)$	0.17	0.06	0.08	0.17	0.05	0.07
FOFB OFF	Yes		0.69	0.47	0.61	0.26	0.21	0.22
Upper bound from Eq. (6)	Yes	0.1	0.50	0.26	0.38	0.26	0.12	0.14
Simulation	Yes	0.1	0.18	0.08	0.09	0.18	0.07	0.09
Upper bound from Eq. (6)	Yes	$f(\theta_i)$	0.50	0.26	0.38	0.26	0.12	0.15
Simulation	Yes	$f(\theta_i)$	0.18	0.08	0.09	0.18	0.07	0.09

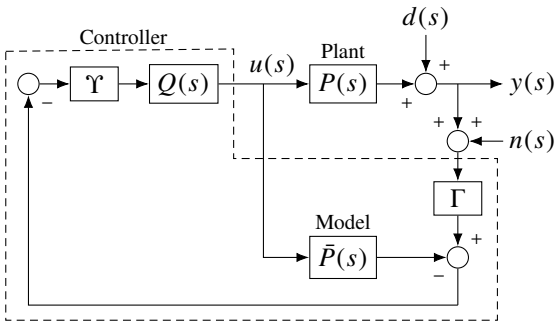

Figure 3: IMC structure with corrector setpoints $u(s)$, disturbances $d(s)$, beam positions $y(s)$, and measurement noise $n(s)$.

corrector inputs, it also reduces the overall bandwidth and therefore the performance at primary BPMs. To improve the performance at primary BPMs, Γ from Eq. (2) is redefined as

$$\Gamma := U \operatorname{diag}\left(\frac{\sigma_1^2}{\sigma_1^2+\mu_1}, \ldots, \frac{\sigma_{n_y}^2}{\sigma_{n_y}^2+\mu_{n_y}}\right) U^{\mathrm{T}}, \tag{3}$$

where $\mu_1, \ldots, \mu_{n_y} \geq 0$ are mode-based regularisation parameters. The mode-based regularisation parameters are defined as $\mu_i = f(\theta_i)$ with

$$\mu_i := \frac{\mu_{\max} - \mu_{\min}}{\theta_{\max} - \theta_{\min}} (\theta_i - \theta_{\min}) + \mu_{\min}, \tag{4}$$

where $\mu_{\min} := 0.01 \leq \mu_i \leq \mu_{\max} := 0.1$, $\theta_{\min} := \min_i \theta_i$, $\theta_{\max} := \max_i \theta_i$, and

$$\theta_i := \operatorname{acos}\left(|w^{\mathrm{T}} U_i| / \|w\|_2\right). \tag{5}$$

The variable θ_i describes the acute angle between U_i, the ith left singular vector of R, and a vector $w \in \mathbb{R}^{n_y}$ with ones at indices of interest and zeroes otherwise. For example, to prioritise primary BPMs, w can be assigned ones at indices corresponding to primary BPMs, lowering the value of μ_i for modes that form a small angle with w and hence increasing the controller gain for these modes. For the following analysis, all primary BPMs are prioritised using Eq. (4), and these results are compared against a regularisation matrix with $\mu_i = 0.1$ for all modes.

In general, large controller gains will result in a high closed-loop bandwidth, whereas small controller gains will result in a low closed-loop bandwidth. Although the regularisation matrix limits the corrector setpoints, it also reduces the bandwidth for modes associated with small singular values, and therefore the overall controller performance. However, if most of the disturbance is concentrated in modes associated with large singular values, the regularisation matrix does not significantly impact the controller performance, such as it is the case for Diamond. Note that this is not the case for the disturbance data from Fig. 1, which lacks phase information.

RESULTS AND DISCUSSION

Because the PSDs from Fig. 1 lack phase information, the performance of the controller is estimated using two different methods. First, assuming that the measurement noise PSD $N_i(\omega)$ and the disturbance PSD $D_i(\omega)$ are uncorrelated, the PSD $Y_i(\omega)$ of BPM i can be upper-bounded by

$$Y_i(\omega) \leq Y_i(\omega)|_D + Y_i(\omega)|_N, \tag{6}$$

where

$$Y_i(\omega)|_D := \left(\sum_{k=1}^{n_y} |S_{ik}(\mathrm{j}\omega)| \sqrt{D_k(\omega)}\right)^2$$

$$Y_i(\omega)|_N := \left(\sum_{k=1}^{n_y} |I - S_{ik}(\mathrm{j}\omega)| \sqrt{N_k(\omega)}\right)^2$$

and $S_{ik}(\mathrm{j}\omega)$ refers to element on row i and column k of the sensitivity, i.e. the transfer functions from disturbance and

ISBN: 978-3-95450-236-3 ISSN: 2673-5350 doi:10.18429/JACoW-IBIC2023-MOP041

noise to the output, which is defined as

$$S(s) := I - P(s)Q(s)\Upsilon(I + (\Gamma - I)P(s)Q(s)\Upsilon)^{-1}\Gamma. \quad (7)$$

Second, the PSDs from Fig. 1 can be used to sample a time series for each BPM by adding a random phase, and the time series can be used in simulations. Although the resulting performance does not represent a strict upper bound, the results can be interpreted as a worst-case scenario. Because the Diamond-II disturbance does not reflect the characteristic distribution in modal space, the regularisation matrix significantly reduces the overall performance.

The integrated beam motions (IBMs) up to 1 kHz obtained from the upper bound using Eq. (6) and the simulations for $\mu_i = f(\theta_i)$ and $\mu_i = 0.1$ are summarised in Table 2, which also shows the corresponding beam stability target. The first part of the table shows the performance without noise, so that FOFB OFF corresponds to the IBM of the disturbance. For both choices of μ_i, the simulation yields significantly better results than the upper bound from Eq. (6). Except for the long straights in the vertical direction, the upper bound is below target, suggesting that the Diamond-II stability specifications are met. Although the primary BPMs are prioritised, the choice $\mu_i = f(\theta_i)$ does not improve the performance, but increases the upper bound from Eq. (6), and leaves the simulation results unchanged. On one hand, this is related to the lack of phase information for the disturbance data from Fig. 1. On the other, these results suggest that decreasing μ_i below $\mu_{\max}$ does not significantly affect the regularisation gains from Eq. (3) and the closed-loop bandwidth, i.e. both $\mu_{\max}$ and $\mu_{\min}$ in Eq. (4) would need to be lowered further to yield a performance increase on primary BPMs. However, this would also increase the corrector demand above the Diamond-II limit of 920 mA.

The second half of Table 2 shows the performance in the presence of measurement noise, so that FOFB OFF corresponds to the IBM obtained after adding $D(\omega)$ and $N(\omega)$. Compared to the case without noise, the IBM for FOFB OFF is ~ 0.01 µm larger. As for the case without noise, the simulations yield significantly better results than the upper bound from Eq. (6), and the different choices of μ_i do not impact the performance. Except for the long straights that are 0.03 µm above target in the vertical direction, the upper bounds from Eq. (6) is within target.

CONCLUSION

With the aim of improving the FOFB performance at primary BPMs, a new regularisation matrix was defined using mode-by-mode regularisation parameters. The regularisation parameters were reduced for those modes that impact the primary BPMs most. The performance of the resulting controller was evaluated using a conservative upper bound and in simulations, and compared against a controller that uses a constant regularisation parameter. Two scenarios were considered, one with measurement noise and disturbance, and one with disturbance only. The measurement noise was modelled based on the specifications for the new Diamond-II electron BPMs.

The simulation results have shown that the Diamond-II specifications are met on all straights for both scenarios, whereas with the upper bound, the IBM on long straights is 0.03 µm above target. For both simulations and upper bounds, the new mode-by-mode regularisation matrix has not led to any performance improvements. It remains unclear why, but it is suspected that the lack of phase information for the Diamond-II disturbance data impacts the regularisation and the resulting performance.

On-going work at Diamond is reassessing the slow and fast corrector demand using the new disturbance data and the new measurement model. In addition, the fast corrector models will be updated once they are prototyped.

Future research could analyse the impact of the regularisation matrix in more detail, e.g. by considering a robust performance criteria in modal space and or by modifying the controller dynamics in generalised modal space. In addition, the results could be reassessed using disturbance data that reflects the characteristic modal distribution.

REFERENCES

[1] S. Gayadeen and S. R. Duncan, "Design of an electron beam stabilisation controller for a synchrotron," *Contr. Eng. Pract.*, vol. 26, pp. 201–210, May 2014. doi:10.1016/j.conengprac.2014.01.012

[2] M. G. Abbott *et al.*, "Diamond-II technical design report," Diamond Light Source, Tech. Rep., Aug. 2022. https://www.diamond.ac.uk/Home/News/LatestNews/2022/14-10-22.html

[3] I. Kempf, P. J. Goulart, and S. Duncan, "Control of Two-Array Cross-Directional Systems using the Generalised Singular Value Decomposition," *arXiv*, doi:10.48550/arXiv.2308.08631

[4] G. H. Golub and C. F. Van Loan, *Matrix Computations*, 4th ed. The Johns Hopkins Univ. Press, 2013.

[5] S. Gayadeen and W. Heath, "An internal model control approach to mid-ranging control," in *Proc. IFAC Symp. Adv. Contr. Chem. Process*, Jul. 2009, pp. 542–547.

[6] I. P. S. Martin *et al.*, "Orbit Stability Studies for the Diamond-II Storage Ring," in *Proc. Int. Part. Accel. Conf. (IPAC'22)*, Bangkok, Thailand, Jul. 2022, pp. 2602–2605. doi:10.18429/JACoW-IPAC2022-THPOPT017

[7] L. T. Stant *et al.*, "Diamond-II Electron Beam Position Monitor Development," in *Proc. IBIC'22*, Kraków, Poland, Dec. 2022, pp. 168–172. doi:10.18429/JACoW-IBIC2022-MO3C2

[8] I. Kempf, M. Abbott, L. Bobb, G. B. Christian, G. Rehm, and S. Duncan, "Fast Orbit Feedback for Diamond-II," presented at IBIC'22, Saskatoon, Canada, this conference.

[9] S. Gayadeen, S. R. Duncan, and G. Rehm, "Optimal control of perturbed static systems for synchrotron electron beam stabilisation," *IFAC PapersOnLine*, vol. 50, no. 1, pp. 9967–9972, 2017, 20th IFAC World Congress.